Supporting Information

Khalaj et al. 10.1073/pnas.1311763110

SI Methods

Genotyping. DNA was acquired via tail biopsy, and total RNA was isolated and purified using RNeasy Mini Kit (Qiagen) and resuspended in RNase-free H_2O (Ambion) and oligo(dT)12–18, as in ref. 1. Standard 30-cycle PCR was performed using the following oligonucleotides to probe for estrogen receptor β (ERβ) loxP: ACG222 (5′-CTTCTTAGAGGTACGGATCCCAGCCC-AGCC-3′) and ACZ310 (5′-AATCTCTTTGCCTTCCAGAGC-TA-3′) (1).

PCR and gel electrophoresis resulted in a 180-bp fragment for WT and 230-bp fragment for loxP. More specifically, PCR yielded a 180-bp fragment for $ER\beta^{+/+}$ (homozygous WT), a 230-bp fragment for homozygous $ER\beta^{fl/fl}$ (loxP/loxP; floxed), and both 230- and 180-bp fragments for heterozygous $ER\beta^{fl/+}$ mice. In addition, Cre recombinase gene presence was assessed by standard PCR (generic NSE-Cre PCR protocol from Jackson Laboratories). Primers for Cre transgene did not distinguish hemizygous from homozygous animals and produced a ∼100-bp fragment.

Primers used were oIMR1084 (5′-GCGGTCTGGCAGTAAA-AACTATC-3′) and oIMR1085 (5′-GTGAAACAGCATTGCTG-TCACTT-3′). As an internal positive control, we also used primers oIMR7338 (5′-CTAGGCCACAGAATTGAAAGATCT-3′) and oIMR7339 (5′-GTAGGTGGAAATTCTAGCATCATCC-3′) to assess a 324-bp product.

Experimental Autoimmune Encephalomyelitis. Active experimental autoimmune encephalomyelitis (EAE) was induced using myelin oligodendrocyte glycoprotein, amino acids 35–55 ($MOG_{35–55}$), as in refs. 2–4). Mice were immunized with 200 μg $MOG_{35–55}$ in combination with 200 μg *Mycobacterium tuberculosis* in complete Freund's adjuvant. These injections were performed s.c. over the inguinal and axillary draining lymph nodes, with injections performed on one side on postinduction day 0 and the contralateral side on day 7. On days 0 and 2, mice also received an i.p. injection of Pertussis toxin (500 ng per mouse). EAE control animals were injected with everything but $MOG_{35–55}$. All animals were monitored and scored daily for clinical disease severity using the following standard EAE grading scale: 0, unaffected; 1, tail limpness; 2, failure to right upon attempt to roll over; 3, partial hind limb paralysis; 4, complete hind limb paralysis; and 5, moribund. Mice were killed at approximately day 40 after induction. Clinical scores for mice within each treatment group were averaged daily to determine mean clinical scores for each treatment group.

Histopathology, Immunohistochemistry, Western Blot Analysis, and Fluorescent and Electron Microscopy. The following antibodies were used for immunohistochemistry to detect: axons, anti-NF200 (1:500, Millipore and 1:1,000, Sigma-Aldrich), anti-SMI-32, anti-APP (1:1,000, Abcam); astrocytes, anti-GFAP (1:1,000, Millipore); oligodendrocyte progenitor cells (OLPs), anti-PDGFRα/anti-olig2 + anti-Ki67 (1:500, Millipore); mature oligodendrocytes (OLs), anti-CC1 (1:1,000, GeneTex), PLP_EGFP fluorescence; myelin, anti-myelin basic protein (MBP) (1:1,000, Millipore); T cells, anti-CD3 (1:1,000, Abcam); microglia/macrophage/monocyte, anti-CD45 (1:1,000, PharMingen); and estrogen receptor β, anti-ERβ (rabbit monoclonal clone 68–4, catalog no. 05–824; 1:1,000, Millipore; and mouse monoclonal catalog no. GTX70174; 1:1,250, GeneTex). The second antibody step was performed by labeling with antibodies conjugated to Cy3 and Cy5 (1:1,000, Vector Laboratories and Chemicon). IgG-control experiments were performed for all primary antibodies, and no staining was observed under these conditions. To assess cell numbers, DAPI (2 ng/mL; Molecular Probes) was added to tissue sections for 10 min before final washes after secondary antibody addition. The sections were mounted on Superfrost slides (VWR), allowed to dry, and coverslipped in Fluoromount G (Fisher Scientific).

For Western blot analysis, the following primary antibodies were used to assess second messenger signaling in spinal cord lysates: rabbit anti-BDNF (Santa Cruz Biotechnology, 14 kDa); mouse anti-GAPDH (Ambion, 1:20,000; 36 kDa); anti-serine-threonine-specific protein kinase (Akt) (60 kDa); anti-Phospho-AKT (Thr308, 60 kDa); anti-mammalian target of rapamycin (mTOR) (289 kDa); anti-Phospho-mTOR (ser-2448; 290 kDa) (Cell Signaling). Band density was determined as scanning units, and expression levels were quantified compared with the levels of GAPDH. Western analysis figures represent a gel containing six to seven lanes. Each lane represents an individual animal within the treatment group. Quantification graphs include four to eight animals per treatment group pooled over two to three separate experiments.

For EM, formalin- and glutaraldehyde-perfused brains were cut sagittally. The genu area of corpus callosum (CC) was identified under a dissecting microscope, and 4-mm^2 blocks [from the mid CC up to one-third splenium, corresponding to the CC area of plates 40–48 (5)] were carefully dissected. These blocks were further cut in 1-mm sections for Epon embedding.

Stereological and g-Ratio Analysis. Immunostaining was quantified using unbiased stereology as in ref. 4. All images (RGB) were converted to grayscale, split, and separated by color channel using ImageJ version 1.29 [Windows version of National Institutes of Health (NIH) ImageJ; downloaded from http://rsbweb.nih.gov/ij/]. To avoid experimenter bias, autoadjustment of brightness and contrast, as well as threshold of staining signal, was carried out by NIH software (refer to Fig. 4 *B*, *v* for areas of the spinal cord). A Grid Plug-in (ImageJ) was used for counting points per area of interest. Pixel intensity of microglia/macrophage activation (a-dorsal column, DC), myelin (a-DC), and $GFAP^+$ (a-DC) staining intensity within the DC of the spinal cord were also measured as percent area of immunoreactivity using ImageJ and were then recorded and compared statistically. All pixel intensities were measured and compared using ×10 and ×40 magnified images. A grid was used to count all axons ($NF200^+$) and myelinated axons (MBP^+ ring around $NF200^+$ axons) per area in the ventral column (c-VC) of coronal spinal cord sections. $Olig2^+$ and $CC1^+$ OLs in the dorsal column (b-DC) of thoracic spinal cord sections were also quantified.

For EM analysis, serial ultrathin sections of CC embedded in Epon were stained with uranyl acetate-lead citrate and analyzed as in ref. 3). Images (×3,600 and ×14,000 magnification) were analyzed using ImageJ. A grid was used to count axons per area of interest. The ratio of axon diameter to total fiber diameter (g-ratio) was measured by dividing the circumference of an axon without myelin by the circumference of the same axon including myelin (3). For most axons, two encounters were measured. At least 400 axons were analyzed per genotype and/or treatment group.

1. Antal MC, Krust A, Chambon P, Mark M (2008) Sterility and absence of histopathological defects in nonreproductive organs of a mouse ERbeta-null mutant. *Proc Natl Acad Sci USA* 105(7):2433–2438.

2. Tiwari-Woodruff S, Morales LB, Lee R, Voskuhl RR (2007) Differential neuroprotective and antiinflammatory effects of estrogen receptor (ER)alpha and ERbeta ligand treatment. *Proc Natl Acad Sci USA* 104(37):14813–14818.

3. Crawford DK, et al. (2010) Oestrogen receptor beta ligand: A novel treatment to enhance endogenous functional remyelination. *Brain* 133(10):2999–3016.
4. Kumar S, et al. (2013) Estrogen receptor β ligand therapy activates PI3K/Akt/mTOR signaling in oligodendrocytes and promotes remyelination in a mouse model of multiple sclerosis. *Neurobiol Dis* 56:131–144.
5. Crawford DK, Mangiardi M, Xia X, López-Valdés HE, Tiwari-Woodruff SK (2009) Functional recovery of callosal axons following demyelination: a critical window. *Neuroscience* 164(4):1407–1421.

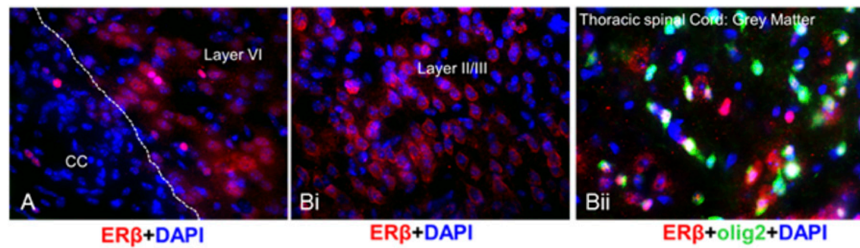

Fig. S1. Visualization of ERβ in various cells within CNS tissue via immunohistochemistry. Coronal sections (40 μm thick) from Formalin-perfused brains of naïve WT animals were treated with 2 N HCl for 10 min, permeabilized using 0.2% Triton X-100 for 30 min, and blocked for 2 h with 20% normal goat serum. (*A*) Mouse monoclonal or (*B*, *i* and *ii*) rabbit monoclonal primary anti-ERβ was added overnight, removed, and, after multiple washes, fluorescently tagged secondary antibody was added. Some sections (*B*, *ii*) were immediately stained with anti-olig2 followed by second secondary antibody and DAPI. As shown in *A* and *B*, *i*, cortical layers reveal strong ERβ staining in the neuronal population. *B*, *ii* shows a representative coronal section of thoracic spinal cord, in which neuronal and OL populations are evident. All images are at ×40 magnification. In sum, the two different ERβ antibodies allow for effective visualization of the receptor in OLs, as well as other cell types (i.e., neurons).

Fig. S2. No gross phenotype in central nervous system myelination of Olig2,ERβ CKO mice compared with littermate controls. (*A*) Costaining with MBP (green) and neurofilament 200 (NF200; red) reveals no difference in MBP intensity and NF200 between Olig2,ERβ CKO and littermate control mice in the cingulum (cg) and corpus callosum (CC). Representative images shown at ×10 magnification. (Scale bar, 100 μm.) (*B*) EM reveals no difference in myelinated axon numbers or g-ratio, with Olig2,ERβ CKO and littermate control mice exhibiting a g-ratio of 0.86 ± 0.006 and 0.87 ± 0.002, respectively. Representative electron micrographs of CC axons shown at ×14,000 magnification. A minimum of 400 fibers were measured from each mouse. (Scale bar, 1 μm.) (*C*) Representative images of mature OLs stained with adenomatous polyposis coli APC (CC1; *Upper*; red) and cells of OL lineage (Olig2; *Lower*; red) in the dorsal column of spinal cord of Olig2,ERβ CKO and littermate control mice imaged at ×40 magnification. (Scale bar, 10 μm.) (*D*) Quantification reveals no difference in number of $CC1^+$ and $Olig2^+$ cells between Olig2,ERβ CKO and littermate control mice. Stain intensity or cell number per 0.4 mm^2 were quantified for *A* and *C*, and sections were also stained with nuclei-labeling DAPI (blue). Postnatal day (P) 15 female mice; (n = 4 per genotype).